PHYSICAL REVIEW A **70**, 062503 (2004)

2*S* hyperfine structure of atomic deuterium

N. Kolachevsky,* P. Fendel, S. G. Karshenboim,† and T. W. Hänsch‡
Max-Planck-Institut für Quantenoptik, 85748 Garching, Germany

(Received 7 April 2004; revised manuscript received 7 July 2004; published 14 December 2004)

We have measured the frequency splitting between the $(2S, F=1/2)$ and $(2S, F=3/2)$ hyperfine sublevels in atomic deuterium by an optical differential method based on two-photon Doppler-free spectroscopy on a cold atomic beam. The result $f_{\mathrm{HFS}}^{(D)}(2S) = 40\,924\,454(7)$ Hz is the most precise value for this interval to date. In comparison to previous radio-frequency measurements we have improved the accuracy by a factor of 3. The specific combination $D_{21} = 8f_{\mathrm{HFS}}^{(D)}(2S) - f_{\mathrm{HFS}}^{(D)}(1S)$ of metastable and ground state hyperfine frequency intervals in deuterium derived from our measurement agrees well with the value for D_{21} calculated from quantum electrodynamics.

DOI: 10.1103/PhysRevA.70.062503 PACS number(s): 32.10.Fn, 32.30.Jc, 12.20.Fv, 42.62.Fi

I. INTRODUCTION

High-precision measurements in light atomic systems allow accurate tests of quantum electrodynamics (QED). QED calculations enter into a number of fundamental values related to free particles and simple atoms. In conventional atomic systems the accuracy of QED tests is restricted by insufficient knowledge of the nuclear structure, which is the main obstacle on the way to improve theoretical predictions for the Lamb shift and the hyperfine structure in hydrogen (see, e.g., [1,2]).

The leading nuclear size corrections for energy levels are proportional to the squared value of the electron's nonrelativistic wave function at the position of the nucleus $(r=0)$:

$$\Delta E_{\mathrm{nucl}} = A_N |\psi(r=0)|^2, \tag{1}$$

where the coefficient A_N is determined by parameters of the nucleus and does not depend on atomic quantum numbers. For S levels in hydrogenlike systems, the probability density at the origin scales with the principal quantum number n as $|\psi(r=0)|^2 \sim 1/n^3$. Thus, if one considers the difference of two energy levels $n'^3E(n'S) - n^3E(nS)$, the leading contribution of nuclear effects cancels out.

Recently, significant progress in calculations of the

$$D_{21} = 8f_{\mathrm{HFS}}(2S) - f_{\mathrm{HFS}}(1S) \tag{2}$$

difference of the 2*S* and 1*S* hyperfine structure (HFS) interval frequencies in light hydrogenlike atoms has been achieved [3]. Additional state-dependent QED terms in the HFS interval frequency $f_{\mathrm{HFS}}(nS)$ up to the order of α^4 and $\alpha^3 m_e/m_p$, as well as the next-to-leading nuclear structure effects, have been calculated. The accuracy of the theoretical prediction for D_{21} now exceeds the experimental accuracy by more than an order of magnitude. Whereas ground state HFS intervals in such atomic systems are measured extremely precisely [e.g., in hydrogen $f_{\mathrm{HFS}}(1S)$ is known to less than 1 mHz [4]], the absolute accuracy of $f_{\mathrm{HFS}}(2S)$ determinations is orders of magnitude worse and is typically about tens of hertz. For improving the accuracy of QED tests based on D_{21} calculations, it is therefore necessary to reduce the uncertainty of $f_{\mathrm{HFS}}(2S)$.

Experimental values for D_{21} were obtained for hydrogen, deuterium, and the $^3\mathrm{He}^+$ ion, based on 1*S* and 2*S* hyperfine interval measurements [4–11]. Up to now, the highest relative accuracy for the D_{21} difference (0.01 ppm) has been achieved in the $^3\mathrm{He}^+$ ion due to the relatively big HFS interval in this system as well as the possibility to trap it. The study of neutral atoms requires different experimental techniques. Traditionally, 2*S* HFS intervals in hydrogen and deuterium have been measured by microwave spectroscopy on a hot atomic beam in a homogeneous magnetic field [5,6,9]. Since the traditional microwave methods have likely reached their limits, we have been working on an optical determination of the hyperfine interval in the metastable 2*S* state of hydrogen and deuterium.

Applying an optical technique [7], we have recently measured the hyperfine splitting of the 2*S* state of the hydrogen atom. It is based on two-photon spectroscopy on a cold atomic beam shielded from magnetic fields. The 2*S* HFS interval has been determined from the frequency difference of two stable light fields exciting the singlet $(F=0)$ and triplet $(F=1)$ components of the 1*S*-2*S* transition. The differential method cancels a number of systematic effects intrinsic to two-photon spectroscopy and provides a significant increase of absolute accuracy in comparison with optical frequency measurements [12–14].

We have improved this technique and applied it to the spectroscopy of atomic deuterium. Since the hyperfine structure in deuterium is approximately four times smaller than in hydrogen, it is more difficult to achieve a comparable relative accuracy for the D_{21} in deuterium. However, the smaller HFS interval opens a possibility to apply a different measurement technique, which allows the reduction of statistical uncertainty, as well as a more thorough study of systematic effects. The experiment, the results, and the systematic effects are presented in the two following sections while a comparison of theory and experiment is summarized in the concluding part of the paper.

---

*Also at P. N. Lebedev Physics Institute, Moscow, Russia.

†Also at D. I. Mendeleev Institute for Metrology, St. Petersburg, Russia.

‡Also at Ludwig-Maximilians-University, Munich, Germany.

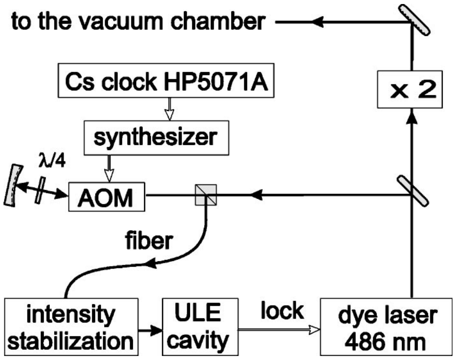

FIG. 1. Laser system for 1*S*-2*S* deuterium spectroscopy.

II. MEASUREMENT OF THE 2*S* HYPERFINE SPLITTING

The 2*S* HFS interval in deuterium has previously been measured by Reich, Heberle, and Kusch [9]. The value of

$$f_{\mathrm{HFS}}^{(D)}(2S) = 40\,924\,439(20)\ \mathrm{Hz} \tag{3}$$

has been obtained by a radio-frequency (rf) method and has not yet been remeasured with comparable accuracy up to now. They used the same method as for an earlier measurement in hydrogen [5]. However, in comparison to the hydrogen measurement, they could improve the absolute accuracy in the determination of $f_{\mathrm{HFS}}^{(D)}(2S)$ by a factor of 3 [9]. In spite of the fact that the HFS intervals in deuterium are more strongly affected by a magnetic field than those in hydrogen, the average of the two rf transition frequencies in the metastable deuterium atom $(F=1/2, m_F=-1/2) \leftrightarrow (F'=3/2, m_F'=1/2)$ and $(F=1/2, m_F=1/2) \leftrightarrow (F'=3/2, m_F'=-1/2)$ contains only quadratic and higher order field-dependent terms and thus is rather insensitive to the field. Still, the most important systematic effects contributing to the 20 Hz uncertainty of this rf technique were the uncertainty in the determination of the magnetic field and the rf Stark effect.

Our result is obtained by a completely different approach, namely, two-photon spectroscopy. To measure the 2*S* HFS interval, we use the hydrogen spectrometer setup described in detail elsewhere [15]. A dye laser operating near 486 nm is locked to a definite TEM_{00} mode of an ultrastable cavity, which is made of an ultralow expansion (ULE) glass and has a drift of less than 0.5 Hz/s (Fig. 1). To change the laser frequency with respect to the cavity mode, we use a broadband double-pass acousto-optic modulator (AOM) placed between the laser and the cavity. The rf synthesizer driving the AOM is continuously referenced to the 10 MHz signal of a HP5071A cesium frequency standard which has a frequency uncertainty that is negligible for the current experiment. After the double-pass AOM, the laser light is spatially filtered by means of a single-mode fiber, while the intensity of the light coupled into the cavity is actively stabilized. By keeping these important coupling conditions constant, we avoid an undesirable frequency shift of the cavity mode, which could result from a change in the intensity or the position of the beam caused by a detuning of the AOM [16].

The frequency of the dye laser is doubled in a barium β-borate crystal, and the resulting 243 nm radiation is coupled into a linear enhancement cavity inside the vacuum chamber where the two-photon excitation takes place.

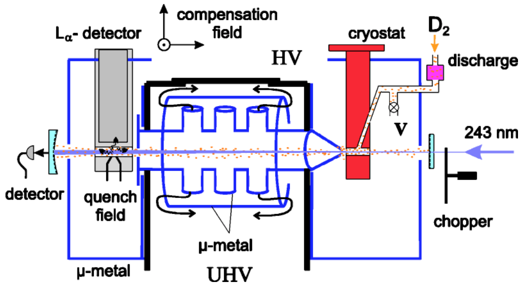

FIG. 2. Vacuum part of the experiment. HV and UHV are the high- and ultrahigh vacuum regions, while *V* is the bypass valve reducing the atomic flow escaping from the nozzle.

Atomic deuterium, produced in a 15 W, 2.5 GHz rf gas discharge, flows through Teflon tubes to a copper nozzle, which is cooled by a flow-through cryostat (Fig. 2). Atoms thermalize with the nozzle walls and then enter the high-vacuum (HV) region of the chamber parallel to the enhancement cavity axis. The HV volume is pumped by a turbomolecular pump to 5×10^{-5} mbar. After about 5 mm the atoms enter an ultrahigh-vacuum (UHV) region which is separated from the HV volume by a 1.5 mm diaphragm. Most of the interaction region (95%) is in this UHV region, which is pumped by a 10^4 l/s cryopump. Without the atomic beam, the background gas pressure in the UHV region equals 3×10^{-8} mbar. The background gas pressure increases with the deuterium flow through the nozzle to a maximum of 2×10^{-7} mbar. A fraction of the atoms traveling along the laser mode is excited to the 2*S* state and then reaches the detection zone where a weak electrical quenching field is applied. The field mixes the 2*S* and 2*P* states of the atoms causing them to decay rapidly to the ground state thereby emitting 121 nm Lyman-α photons. In a time-of-flight measurement scheme, these photons are counted by a solar-blind photomultiplier connected to a photon counter. The excitation radiation is periodically blocked in front of the cavity by a chopper wheel, and 121 nm photons are detected only within a 3 ms dark time interval. Introducing a delay τ between shutting off the light beam and starting the detection, we can thus select different velocity groups contributing to the signal. The delay τ sets an upper limit to the atomic velocity to $v_{\mathrm{max}}=l/\tau$, where l is the distance between the nozzle and detector. Using a multichannel scaler, we sort the counts in adjacent time bins (τ=10, 210, 410 μs,...) and simultaneously record up to 12 spectra containing information about velocity-dependent effects, such as the second-order Doppler effect.

To optimize the spectrometer configuration, which has been used for the recent measurements in atomic hydrogen [7,14], for the current deuterium measurement some important changes have been introduced.

(1) In order to maximize the count rate for slow atoms (with velocities $v\sim200$ m/s) one has to find a compromise between thermalization and recombination processes at the cold walls of the nozzle by adjusting the nozzle geometry and temperature. The best rates are observed with a larger nozzle diameter (2-2.5 mm compared to 1.2 mm for hydro-

gen) and at slightly higher temperatures (6-6.5 K compared to 5 K). Typically, the count rate with the deuterium beam is higher than for hydrogen (by a factor 2-5 depending on τ).

(2) As another improvement, we have installed a bypass valve on the way between the gas discharge and the nozzle, which can be opened to a high-vacuum part of the vacuum chamber (Fig. 2). By opening the valve we reduce the atomic flow through the nozzle by a factor of 4. Even at the lowest pressure in the gas discharge (0.7 mbar) and with the valve opened, the count rate is sufficient to detect a solid 2*S* signal for atoms with $v \sim 200$ m/s.

(3) For better magnetic shielding we have redesigned the inner μ-metal shield. The outer shield together with the compensation magnetic field reduces residual fields over the entire interaction region to 10-20 mG, while the inner shield covering over 90% of the excitation region has the calculated shielding factor of 20 on the axis [7].

(4) The last and most important difference between this and the previous measurement in hydrogen [7] is an adjustment to the electronic laser lock. In the present experiment we are able to alternatingly switch between the two $(1S,F=1/2)\rightarrow(2S,F=1/2)$ (doublet) and $(1S,F=3/2)\rightarrow(2S,F=3/2)$ (quadruplet) transitions in less than 0.2 s by simply changing the AOM frequency (see Fig. 4 below). This allows us to record the two spectra almost simultaneously. Henceforth, this method of simultaneous recording is referred to as the simultaneous method.

To measure the frequency difference between the two two-photon transitions, we have applied the following procedure. We tuned the frequency of the double-pass AOM placed between the reference ULE cavity and the laser to one of the atomic transitions and measured one data point of the spectrum with a photon accumulation time of 0.5 s. After the measurement, the AOM frequency f_{AOM} is swept over a big fixed frequency interval (approximately $[f^{(D)}_{\mathrm{HFS}}(1S)-f^{(D)}_{\mathrm{HFS}}(2S)]/8\approx 36$ MHz) to drive the other two-photon transition. During the sweep, the laser is continuously kept in lock. The factor of 8 arises from the double-pass scheme for the AOM, the second-harmonic generation stage, and the two-photon process. Then we introduce a 0.5 s break as recovery time for multiple feedback loops, and repeat the measurement of one point of the other two-photon transition. After the measurement, in order to scan the frequency of the laser, we add a small frequency step to the frequency of the synthesizer and sweep it back to the first transition. The result of such a procedure is presented in Fig. 3 (top). Both simultaneously recorded doublet and quadruplet transition lines are fitted with a Lorentzian function. To determine the position of the line in the frequency domain a similar fitting procedure is applied with the AOM frequency taken as the x variable. Thus, each recorded transition line can be presented as one point on a time vs f_{AOM} plane as shown in Fig. 3 (bottom). The coordinates of this point are the corresponding centers of the Lorentzian profiles obtained from the fitting procedure.

A typical time interval between the centers of such a doublet/quadruplet line pair is less than 5 s. This corresponds to a small correction on a level of a few hertz, which should be introduced to correct for the reference cavity drift. By using the simultaneous method, the influence of the reference cavity's frequency fluctuations on the 2*S* HFS measurement statistics is significantly reduced. Moreover, it suppresses the influence coming from all drifts in the experimental setup (e.g., drift of the laser lock electronics' zero point or drift of the 243 nm radiation power in the enhancement cavity) with a time scale exceeding 200 s. This is the required time to record a pair of lines. Even though such fluctuations do not introduce systematic shifts, a long time is required to average them. The simultaneous approach is less sensitive to systematic effects: one independent point is obtained after 3 min. of measurement, while for the previous method [7] the corresponding time interval was about 20 min.

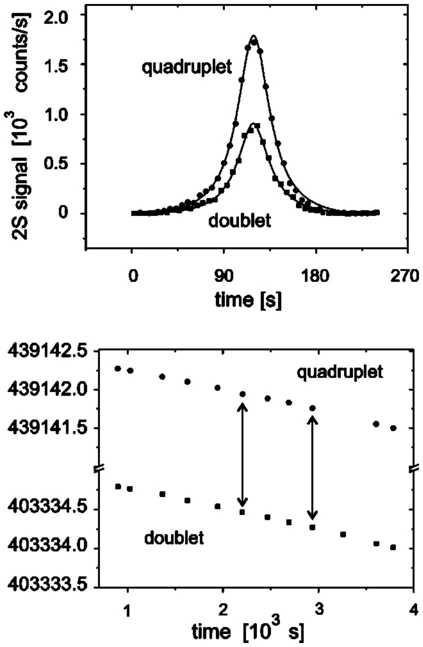

FIG. 3. Simultaneous recording of the two transition lines (top). AOM frequencies f_{AOM} corresponding to the centers of the doublet and quadruplet transition lines fitted by Lorentzian functions. The frequency change is due to the drift of the reference ULE cavity (bottom).

III. RESULTS AND SYSTEMATIC EFFECTS

We have measured $f^{(D)}_{\mathrm{HFS}}(2S)$ during 7 days using the simultaneous method and during 6 days applying the method described in [7]. To test for systematic effects we have varied the deuterium flow (within each day) and the magnetic field. We have recorded over 1000 deuterium time-resolved spectra. The averaged amplitude ratio between quadruplet and doublet transitions equals 2.00(2), which agrees well with the theoretical expectation.

In the absence of magnetic field, the 2*S* HFS interval frequency is given by the following combination of optical frequencies and the ground state HFS interval:

$$f^{(D)}_{\mathrm{HFS}}(2S)=f^{(D)}_{\mathrm{HFS}}(1S)+f_{F=3/2}-f_{F=1/2}, \tag{4}$$

where $f_{F=1/2}$ and $f_{F=3/2}$ are the frequencies of the doublet and the quadruplet transitions at 121 nm (see Fig. 4). The fre-

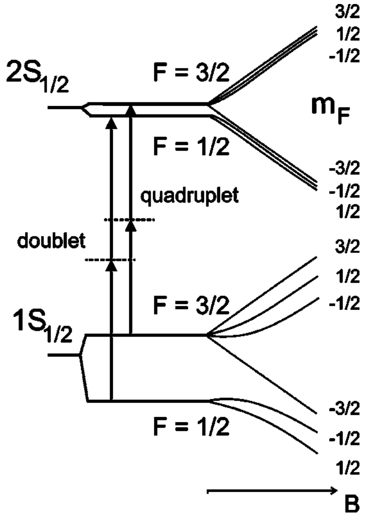

FIG. 4. Two-photon transitions between hyperfine components of the 1*S* and 2*S* levels in atomic deuterium. The spliting of magnetic sublevels in a magnetic field is also presented (not to scale).

quency of the ground state splitting has been measured by Wineland and Ramsey [8] with an uncertainty of 5×10^{-12}:

$$f_{\mathrm{HFS}}^{(D)}(1S) = 327\,384\,352.5222(17)\ \mathrm{Hz}. \tag{5}$$

The contribution to the resulting error budget of $f_{\mathrm{HFS}}^{(D)}(2S)$ introduced by this uncertainty is negligible.

For this differential measurement, the most significant systematic effects of two-photon beam spectroscopy cancel out. As shown in [7], the differential dynamic Stark shift cancels to the level of 10^{-6} relative to the shift of the 1*S*-2*S* transition (about 500 Hz). Because of some residual fluctuations of the 243 nm radiation intensity, the doublet and quadruplet lines acquire slightly different shifts. We correct this difference for each line by monitoring the power leaking out of the cavity (Fig. 2). The resulting correction for the simultaneous method equals 0.5 Hz, which is a factor of 4 lower than for the measurement in hydrogen [7]. For the simultaneous recording technique, long-term intensity fluctuations in the enhancement cavity contribute less to the result than in the case of [7]. In addition to the correction, we add a 0.5 Hz uncertainty.

The contribution of the linear Zeeman effect cancels for allowed two-photon transitions between levels with $\Delta F=0$. The HFS frequency shift in a magnetic field B scales as B^2/f_{HFS}, which is unfavorable for deuterium in comparison to hydrogen. But due to a small magnetic field and the absence of linear terms, our measurement is rather insensitive to magnetic field inhomogeneity, which was crucial for the rf methods. In our case, the magnetic field B shifts the frequency $f_{\mathrm{HFS}}^{(D)}(2S)$ approximately as $35B^2$ kHz/G^2.

A residual magnetic field splits the magnetic sublevels and shifts the measured hyperfine splitting to higher values. The shift mostly originates from imperfectly shielded parts of the excitation region lying in the HV region (Fig. 2). To check for this effect, we conducted one set of measurements without a compensation field and observed a change of $f_{\mathrm{HFS}}^{(D)}(2S)$ equal to 20(22) Hz. Without a compensation field, the measured value of magnetic field around the nozzle and the detector is about 200 mG. The compensation field reduces the total magnetic field by at least a factor of 10, which means that the residual shift should be less than one hertz. We conservatively estimate the shift as 0.5(1.0) Hz.

A dc electrical field E mixes the $2S_{1/2}$ and $2P_{1/2}$ levels causing a 2*S* level shift. According to [17], this energy shift of the 2*S* level is inversely proportional to the Lamb shift. Thus, the differential shift scales as $E_{\mathrm{HFS}}/L_{2S\text{-}2P}$, where $L_{2S\text{-}2P}$ is the Lamb shift of the 2*S* level. The calculated shift of the 2*S* HFS interval in deuterium is about four times smaller than in hydrogen and equals $-300E^2\ \mathrm{Hz\,cm^2/V^2}$. The excitation region is shielded from stray fields by coating all surrounding parts of the interaction region with graphite. The residual stray field in the setup is estimated to be less than 30 mV/cm [18], which corresponds to a 2*S* HFS interval frequency shift of less than −0.3 Hz. We add an uncertainty of 0.5 Hz to the budget of uncertainties taking into account the slightly worse geometrical properties of our shielding compared to the Faraday cage used in [18].

Another source for level shift is a pressure shift caused by collisions with the background gas and within the beam itself. The ground state hyperfine splitting in hydrogen and deuterium is rather insensitive to collisions. Typically, this shift is approximately 1 Hz/mbar depending on the buffer gas [19,20] and thus leads to an extremely small shift for our pressure range. Unfortunately, there is no reliable experimental data for the pressure shift of the 2*S* HFS interval frequency [6,7]. The upper limit for the 2*S* HFS interval frequency shift can be taken as the frequency shift of the $1S(F=1,m_F=\pm1)\rightarrow 2S(F'=1,m_F'=m_F)$ transition, which equals −8(2) MHz/mbar [21,22]. However, considering theoretical work presented in [23,24], there is no reason to expect the shift of the 2*S* HFS interval frequency to be orders of magnitude higher than for the ground state.

We have experimentally investigated the influence of collisions on the $f_{\mathrm{HFS}}^{(D)}(2S)$ frequency. Most of the collisions take place within the atomic beam where the pressure can be much higher than the background gas pressure. Using the method of simultaneous detection, we have varied the atomic flow over a wide range by changing the pressure in the gas discharge (between 0.8 mbar and 8 mbar) and by opening the bypass valve (Fig. 2). The background gas pressure scales linearly with the flow and has a small offset of 3×10^{-8} mbar. Experimental data are presented in Fig. 5. Each point represents the result of statistical averaging of multiple data points detected on different days. About 1/4 of all the data were taken at the lowest pressure in the gas discharge and with an opened valve (the left black point). At high flows, the slow atoms are accelerated and pushed away from the beam by collisions (Zacharias effect) [18]. This causes a loss in statistics and a corresponding increase of uncertainty. Moreover, a fast growth of a film of molecular deuterium on the nozzle restricts the measurement time. For the previous method [7], a flow range of more than 2 units (Fig. 5) was practically unreachable. On our level of accuracy we have not observed any indication for a 2*S* HFS interval pressure shift.

The observed transition lines are shifted by the second-order Doppler effect in a range between 0.1 and 1 kHz de-

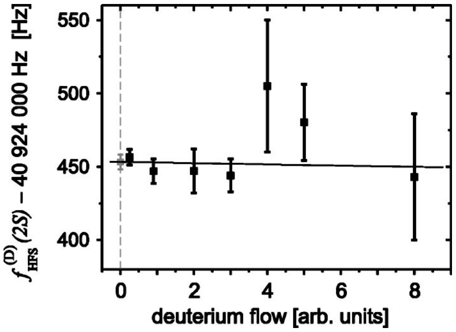

FIG. 5. The 2*S* HFS frequency vs deuterium flow. One unit corresponds to 3.6×10^{17} particles coming to the nozzle per second. The data are obtained using the simultaneous recording method and correspond to the delay time of $\tau=410$ μs. To extrapolate to zero flow (gray point) we fitted the data with a linear function (solid line).

pending on the velocity distribution of the atoms contributing to the signal [13]. The lines are not symmetric and significantly differ from Lorentzian profiles at short ($\tau < 410$ μs) delays (Fig. 6). However, the two-photon transitions are excited in the same thermal beam and the signal is detected with some precisely defined delay time τ, *equal* for both doublet and quadruplet transitions. Therefore, the shift and the influence of the asymmetry, which is spin independent, substantially cancel out. To prove this and to check for possible signal-intensity-dependent or velocity-dependent effects, we evaluated the $f^{(D)}_{\rm HFS}(2S)$ frequency for various delays. After the data for each delay were corrected for the ac Stark shift, the extrapolation to zero flow was made (Fig. 5). The results of this extrapolation are presented in Table I. All velocity-dependent systematic effects, if they exist, should reveal themselves in such an evaluation procedure. Since all results are consistent within the error bars, we believe that the error caused by using a Lorentzian fit instead of a complicated seven-parameter line form model [25] is negligible.

For higher delays τ, the uncertainty grows due to the lack of statistics. The final result of $f^{(D)}_{\rm HFS}(2S)=40\,924\,453(6)$ Hz is obtained by choosing τ to be 410 μs. This choice of τ was made for the following reasons: (i) the statistical uncertainty for this result is small, (ii) the line profile is practically indistinguishable from a Lorentzian, and (iii) the fast nonthermalized atoms do not contribute to the signal. We add an additional uncertainty of 0.3 Hz corresponding to the conservatively estimated shift coming from the collisions with the residual background gas.

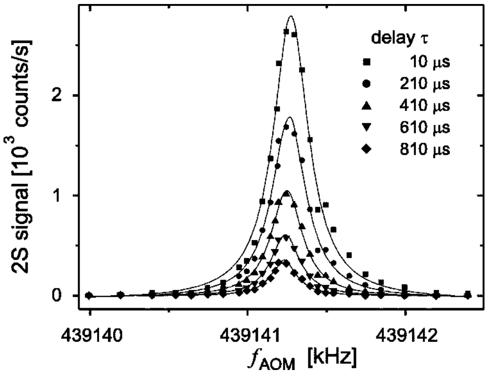

FIG. 6. Quadruplet transition lines and corresponding Lorentzian fits for the different delays τ. Although the lines detected for $\tau=10$ and 210 μs are visibly asymmetrical, the line asymmetry decreases at higher delays.

TABLE I. 2*S* HFS frequency and statistical uncertainty of extrapolation for different delays τ. The velocity $v_{\rm max}$ represents the maximal velocity of atoms contributing to the signal. The coefficient *k* is the slope of the linear fit (Fig. 5).

τ (μs)	$v_{\rm max}$ (m/s)	$f^{(D)}_{\rm HFS}(2S)$ (Hz)	*k* (Hz/arb. units)
10		40 924 452(7)	4(4)
210	1000	40 924 454(3)	0.6(2.0)
410	510	40 924 453(6)	−0.4(3.0)
610	340	40 924 448(10)	0.3(6.0)
810	260	40 924 446(15)	−5(9)

The data obtained during 6 days of measurement applying the method presented in [7] give the result of $f^{(D)}_{\rm HFS}(2S)=40\,924\,462(15)$ Hz, which is perfectly consistent with the one obtained by the simultaneous method. The data are taken only from measurements with low deuterium flows (0.2–1.5 units) (see Fig. 5) and are simply averaged over the entire ensemble. We have increased the uncertainty due to a possible pressure shift (1 Hz) and an ac Stark shift (2 Hz).

Combining these two statistically independent results and adding all known systematic uncertainties linearly, we arrive at the final value for the 2*S* hyperfine interval in atomic deuterium:

$$f^{(D)}_{\rm HFS}(2S) = 40\,924\,454(7)\ \text{Hz}. \tag{6}$$

This result is in good agreement with the one obtained by a rf method [9], but is three times more accurate. The results as well as the budget of uncertainties are collected in Table II.

TABLE II. Summary of systematic uncertainties and the final result for the 2*S* hyperfine interval. The independent results obtained by the simultaneous recording method and the one from [7] are presented.

	Contribution (Hz)	Uncertainty (Hz)
Simultaneous method	40 924 453	6
ac Stark shift		0.5
dc Stark shift	−0.3	0.5
Magnetic field	0.5	1.0
Pressure shift		0.3
Method of [7]	40 924 462	15
ac Stark shift		2
dc Stark shift	−0.3	0.5
Magnetic field	0.5	1.0
Pressure shift		1
Result	40 924 454	7

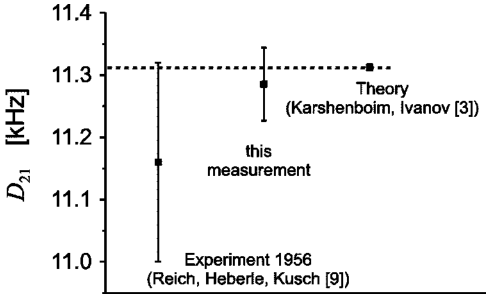

FIG. 7. Experimental and theoretical values for D_{21} in deuterium. The dashed lines represent the uncertainty of the theoretical value.

IV. D_{21} DIFFERENCE

To derive the D_{21} difference we need to combine our result with the known value of the 1*S* HFS interval [8]

$$D_{21} = 8 f^{(D)}_{\mathrm{HFS}}(2S) - f^{(D)}_{\mathrm{HFS}}(1S) = 11\,280(56)\ \mathrm{Hz}. \tag{7}$$

This result agrees well with the theoretical prediction [3]

$$D^{\mathrm{theor}}_{21} = 11\,312.5(5)\ \mathrm{Hz}. \tag{8}$$

The experimental and theoretical values are presented in Fig. 7. The accuracy of our result allows for a test of the state-dependent QED contributions at the level of 0.2 ppm, which can be compared to similar tests in hydrogen [7] and the $^3\mathrm{He}^+$ ion [11]. We point out that the absolute accuracy of our measurement exceeds both cited results, while the relative accuracy suffers from the relatively small HFS interval in deuterium.

After a successful measurement of the Lamb shift [13,26] and the 2*S* HFS interval in the hydrogen atom [7] we have now presented a result for the 2*S* HFS interval in deuterium with an accuracy exceeding that of rf methods.

The accuracy of the optical measurement can be improved by further reducing the atomic velocity. The current results indicate that the pressure shift, which limits the accuracy of absolute frequency measurements in ultracold hydrogen [22], may not play such a crucial role for the differential technique.

ACKNOWLEDGMENTS

The work was partially supported by DFG (Grant No. 436RUS113/769/0-1) and RFBR (Grants No. 03-02-04029 and No. 04-02-17443). The authors wish to thank U. Jentschura, Th. Udem, and M. Fischer for useful discussions and M. Herrmann and T. Nebel for their careful reading of the manuscript.

---

[1] M. I. Eides, H. Grotch, and V. A. Shelyuto, Phys. Rep. **342**, 63 (2001).
[2] S. G. Karshenboim, in *Precision Physics of Simple Atomic Systems*, edited by S. G. Karshenboim and V. B. Smirnov (Springer, Berlin, 2001), p. 141.
[3] S. G. Karshenboim and V. G. Ivanov, Phys. Lett. B **524**, 259 (2002); Eur. Phys. J. D **19**, 13 (2002).
[4] N. Ramsey, in *Quantum Electrodynamics*, edited by T. Kinoshita (World Scientific, Singapore, 1990), p. 673; Hyperfine Interact. **81**, 97 (1993).
[5] J. W. Heberle, H. A. Reich, and P. Kusch, Phys. Rev. **101**, 612 (1956).
[6] N. E. Rothery and E. A. Hessels, Phys. Rev. A **61**, 044501 (2000).
[7] N. Kolachevsky *et al.*, Phys. Rev. Lett. **92**, 033003 (2004).
[8] D. J. Wineland and N. F. Ramsey, Phys. Rev. A **5**, 821 (1972).
[9] H. A. Reich, J. W. Heberle, and P. Kusch, Phys. Rev. **104**, 1585 (1956).
[10] H. A. Schluesser *et al.*, Phys. Rev. **187**, 5 (1969).
[11] M. H. Prior and E. C. Wang, Phys. Rev. A **16**, 6 (1977).
[12] M. Niering *et al.*, Phys. Rev. Lett. **84**, 5496 (2000).
[13] F. Biraben *et al.*, in *The Hydrogen Atom: Precision Physics of Simple Atomic Systems*, edited by S. G. Karshenboim *et al.* (Springer, Berlin, 2001), p. 17.
[14] M. Fischer *et al.*, Phys. Rev. Lett. **92**, 230802 (2004).
[15] M. Fischer *et al.*, Can. J. Phys. **80**, 1225 (2002).
[16] A. Yu. Nevsky, M. Eichenseer, J. von Zanthier, and H. Walther, Opt. Commun. **210**, 91 (2002).
[17] H. A. Bethe and E. E. Salpeter, *Quantum Mechanics of One- and Two-Electron Atoms* (Plenum, New York, 1977).
[18] A. Huber *et al.*, Phys. Rev. A **59**, 1844 (1999).
[19] L. W. Anderson, F. M. Pipkin, and J. C. Baird, Phys. Rev. Lett. **4**, 69 (1960).
[20] C. L. Morgan and E. S. Ensberg, Phys. Rev. A **7**, 1494 (1973).
[21] D. H. McIntyre *et al.*, Phys. Rev. A **41**, 4632 (1990).
[22] Th. C. Killian *et al.*, Phys. Rev. Lett. **81**, 3807 (1998).
[23] W. D. Davison, J. Phys. B **2**, 1110 (1969).
[24] S. Ray, J. D. Lyons, and T. P. Das, Phys. Rev. **174**, 104 (1968).
[25] A. Huber, B. Gross, M. Weitz, and T. W. Hänsch, Phys. Rev. A **59**, 1844 (1999).
[26] M. Weitz, F. Schmidt-Kaler, and T. W. Hänsch, Phys. Rev. Lett. **68**, 1120 (1992).